

Controlling the Morphology of Ag Nanoclusters by Ion Implantation to Different Doses and Subsequent Annealing

Feng Ren, Changzhong Jiang,* Chang Liu, and Jianbo Wang

Key Laboratory of Acoustic and Photonic Materials and Devices of Ministry of Education, Wuhan University, Wuhan 430072, China
Department of Physics, Wuhan University, Wuhan 430072, China

Takeo Oku

Institute of Scientific and Industrial Research, Osaka University, Mihogaoka 8-1, Ibaraki, Osaka 567-0047, Japan

(Received 28 April 2006; revised manuscript received 22 June 2006; published 16 October 2006)

Ag ions were implanted at 200 keV into silica with nominal doses ranging from 5×10^{16} to 2×10^{17} ions/cm². We find that nanovoid-containing Ag nanoclusters form in the implanted samples with doses higher than 1×10^{17} ions/cm². When the dose is increased to 2×10^{17} ions/cm², the nanovoids gradually shrink and form a sandwiched nanocluster-nanovoid-nanocluster structure. The evolution of sandwiched nanoclusters during annealing was observed by *in situ* transmission electron microscopy experiments. Potential mechanisms for the formation and evolution of the irradiation-induced nanovoids and the sandwiched structure nanoclusters with increasing doses are discussed. The structural optimization of the sandwiched structure nanoclusters was performed by molecular mechanics calculations.

DOI: [10.1103/PhysRevLett.97.165501](https://doi.org/10.1103/PhysRevLett.97.165501)

PACS numbers: 61.72.Ww, 61.72.Qq

Recently, nanoclusters with novel topologies, such as core-shell, hollow, multilayer, triangular nanocluster, have received considerable attention owing to their interesting morphologies, specific structures, and good optical, electric, or magnetic properties [1–4]. Ion-beam-based techniques (e.g., ion implantation, ion irradiation) have proven to be versatile and powerful in synthesizing and tailoring nanocluster composites due to their nonequilibrium atomic injection beyond the solubility limit and excellent controllability of ion energy, mass, dose, etc. [5–10]. Meldrum *et al.* [11] observed the nanovoids in metal nanoclusters formed by ion implantation and subsequent annealing at a temperature higher than the corresponding bulk boiling points of the implanted elements. This phenomenon was attributed to the volume contraction during the solidification of the nanoclusters and the migration of implanted elements. Recently, we have observed that the nanovoids in nanoclusters formed by Cu ion implantation into silica evolve into different morphologies during subsequent annealing [12]. The evolution may provide a great opportunity for producing novel nanostructures. However, little attention has been paid to the evolution of these nanoclusters with increasing dose and the irradiation effect of self-ions on the implantation-induced metal nanoclusters. This is important for the properties of nanocluster composites and was often neglected.

In this Letter, we report on controlling the morphology of Ag nanoclusters by high-dose Ag⁺ implantation into silica and subsequent annealing. We find that nanovoid-containing Ag nanoclusters with a set of satellite nanoclusters are formed when the dose reaches 1×10^{17} ions/cm², which changes to sandwiched nanocluster-nanovoid-nanocluster structure nanoclusters after increasing the dose to 2×10^{17} ions/cm². The molecular mechanics calculations show that the sandwiched

structure is stable. This structure disappears after the sample is annealed *in situ* in a TEM at 600 °C.

Highly-purity silica slides were implanted at room temperature by silver ions at 200 keV. The nominal doses were 5×10^{16} , 1×10^{17} , and 2×10^{17} ions/cm², respectively. The current densities of ion implantation are lower than $2.5 \mu\text{A}/\text{cm}^2$ for all the samples. The implanted samples were examined using a JEOL 2010 (HT) transmission electron microscope (TEM) with maximal tilting angles of $\pm 40^\circ$ and a JEOL 2010FEF (UHR) microscopy equipped with an omega energy filter. The structural optimization of the Ag nanoclusters was performed by molecular mechanics calculations (MM2) using CS Chem3D Ultra (CambridgeSoft, MA, USA).

Figure 1 shows the cross-sectional and planar TEM images of the samples implanted by 5×10^{16} (a),(c) and 1×10^{17} (b),(d) Ag⁺ ions/cm². Ag nanoclusters are clearly seen in Fig. 1(a). As a fast diffusing element, Ag atoms aggregate easily into large nanoclusters. Interestingly, the nanoclusters with bright contrast in their centers were seen in Figs. 1(b) (taken by tilting the sample for 20°) and 1(d). The bright contrast always exists when the sample was tilted from 0 to $\pm 40^\circ$, indicating that the bright contrast is not produced due to diffraction contrast, or overlap. The selected area electron diffraction (SAED) pattern [inset in Fig. 1(b)] and the high-resolution TEM image (not shown here) both show the single fcc phase of Ag.

Another obvious feature appearing in the planar TEM image of the sample implanted by 1×10^{17} Ag⁺ ions/cm² is that the large Ag nanoclusters with bright central contrast are surrounded by a set of small satellite nanoclusters. Similar phenomenon was also found by irradiation of nanoclusters or multilayer films with different kinds of ions [6,7,13,14]. The ballistic process induced by the col-

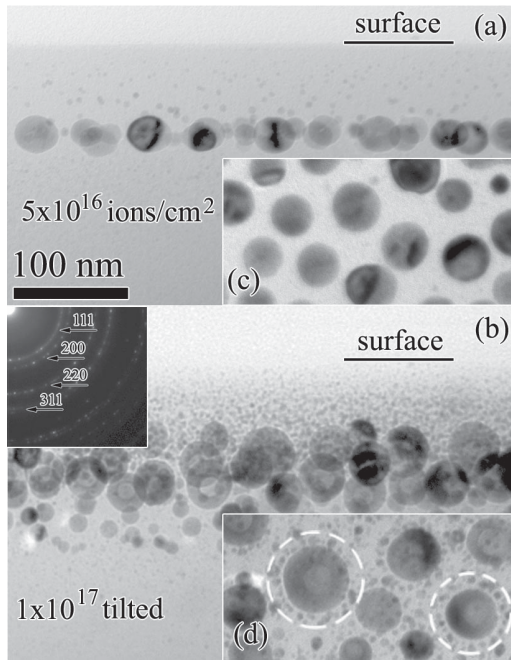


FIG. 1. Cross-sectional, planar TEM images of the samples implanted by 200 keV, 5×10^{16} (a), (c) and 1×10^{17} (b), (d) Ag^+ ions/ cm^2 , and the SAED pattern [inset] for the sample implanted by 1×10^{17} Ag^+ ions/ cm^2 .

lision cascades and the ejection of atoms from nanoclusters are attributed to the formation of satellite nanoclusters [13]. This process involves with the formation of vacancies. For nanoscale clusters in silica, it is easy to reach a high density of vacancies under high-dose ion irradiation, because they do not easily diffuse into the surrounding amorphous matrix. When the density of vacancies becomes supersaturated, these vacancies aggregate into nanovoids, driven by the heat produced by the electronic fraction of the energy loss to reduce its surface energy. By comparing the TEM images shown in Fig. 1(b) with Fig. 1(a), it is seen that new nanoclusters were formed below the large ones with the increase of dose, which indicates that the formed nanoclusters were indeed irradiated by subsequently implanted Ag ions. Therefore, the nanovoids were formed in Ag nanoclusters by ion implantation to a dose of 1×10^{17} ions/ cm^2 due to the aggregation of vacancies produced during ion implantation. The formation, growth, and shrinkage of nanovoids in Cu nanoclusters had been observed by high-dose ion implantation and following annealing [12].

We further study the evolution of nanovoids with the increase of the Ag^+ ions dose. Figures 2(a) and 2(b) show the cross-sectional and planar TEM images for the sample implanted by 2×10^{17} Ag^+ ions/ cm^2 . Interestingly, we find that a sandwiched nanocluster-nanovoid-nanocluster structure was formed, as indicated by arrows in Figs. 2(a) and 2(b). These sandwiched nanocluster structures are similar to the crust-mantle-core structure of the earth. Such sandwiched structure was predicted by Zhu [15].

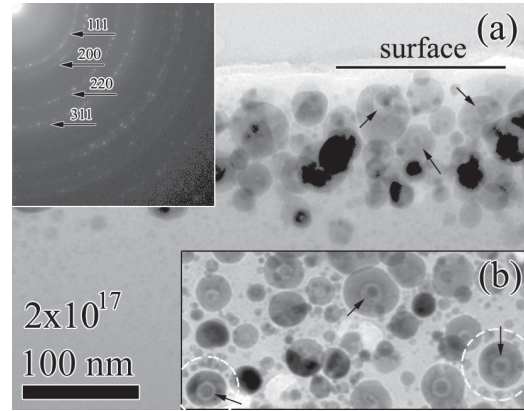


FIG. 2. Cross-sectional (a), planar (b) TEM images, and SAED pattern [inset] for the sample implanted by 200 keV, 2×10^{17} Ag^+ ions/ cm^2 .

The SAED pattern taken from the planar view [inset in Fig. 2(b)], also shows the single fcc phase of Ag. Therefore, the formation of new phases can be excluded and the small nanoclusters in the nanovoids should also be Ag nanoclusters. The STEM-HAADF image for a sandwiched structure nanocluster is shown in Fig. 3(a). Figure 3(b) shows two line scanned average atomic number profiles crossing a sandwich structure nanocluster and a solid nanocluster with close size. It can be found that the average atomic number through the middle layer of the sandwiched structure nanocluster is much lower than that through the core and shell layer. Therefore, the formation of nanovoids in nanoclusters is confirmed once again.

The capture of metal or noble gas atoms in fullerenes by ion implantation into fullerenes had been well observed [16–18]. The atoms keep in stable formation due to van der Waals or electrostatic interaction depending on the category of inner atoms. The formation process of endohedral fullerenes was simulated by *ab initio* molecular dynamics, which indicated that only the atoms with suitable energy could be captured by fullerenes. The appearance of nanoclusters in nanovoids is possibly related to the similar process that some penetrated Ag atoms with low kinetic energy or/and the Ag atoms from the inner walls which are bombarded into the nanovoids by subsequently implanted self-ions, were captured by the nanovoids and aggregated into Ag nanoclusters. These small nanoclusters stay in the nanovoids by electrostatic interaction with the inner walls of nanovoids. Therefore, the nanovoids in Ag nanoclusters are very efficient capturing sites for the self-atoms.

Atomic structure models for Ag_{12} with 12 atoms and $\text{Ag}_{160}(\text{I})$ nanoclusters with 160 atoms were constructed to investigate the stability of the Ag nanoclusters, as shown in Figs. 4(a) and 4(b), respectively. The sizes of the Ag_{12} and $\text{Ag}_{160}(\text{I})$ nanoclusters are 0.56 and 1.95 nm, respectively. In addition, the Ag_{160} nanocluster with the fcc structure has an inner nanovoid in the center. The size of the nanovoid is 1.46 nm. The nanovoid and $\text{Ag}_{160}(\text{I})$ are concentric. Then,

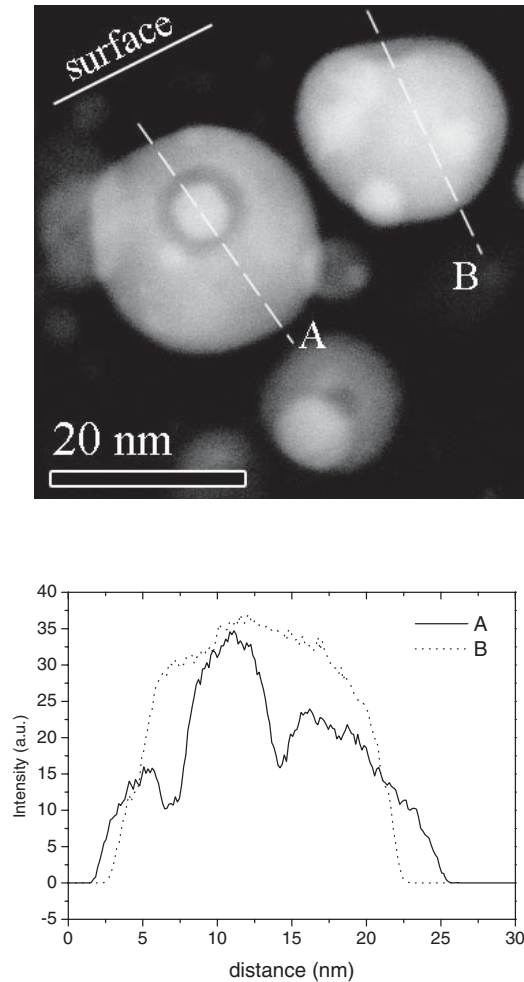


FIG. 3. Cross-sectional STEM-HAADF image for the sample implanted by 200 keV, 2×10^{17} Ag^+ ions/ cm^2 , and two line scanned average atomic number profiles crossing a sandwich structure nanocluster and a solid nanocluster.

the Ag_{12} was introduced inside the Ag_{160} (I), as shown in Fig. 4(c). As observed from the TEM images, there are 30% nanovoids with their centers shifted from the centers of the nanoclusters. Therefore, atomic structure models for Ag_{160} (II) nanoclusters with the center of the nanovoid shifted 0.07 nm were also constructed, as shown in Fig. 4(e). After molecular mechanics calculation, the structure of $\text{Ag}_{12}@Ag_{160}$ (I) and $\text{Ag}_{12}@Ag_{160}$ (II) were optimized, and both the Ag_{12} were centered in the Ag_{160} , as shown in Figs. 4(d) and 4(f). The total energies of

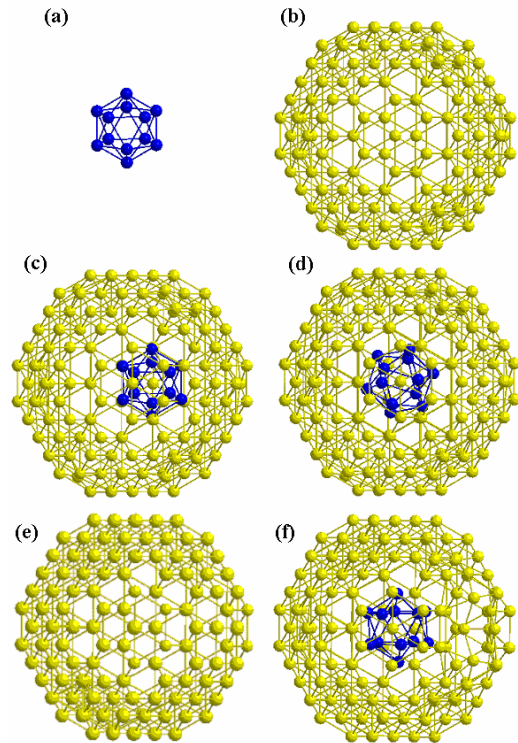


FIG. 4 (color online). Atomic structure models for (a) Ag_{12} , (b) Ag_{160} (I) nanoclusters, and (e) Ag_{160} (II) after molecular mechanics calculation. (c),(d) Structure models for $\text{Ag}_{12}@Ag_{160}$ (I) before and after calculation, respectively. (f) Structure models for $\text{Ag}_{12}@Ag_{160}$ (II) after calculation. After calculations, the structures are optimized.

$\text{Ag}_{12}@Ag_{160}$ were reduced after calculation, as given in Table I, which indicates the Ag_{160} nanovoid structure was stabilized by introducing Ag_{12} nanocluster. The energy increases when the void is shifted from the center, which indicates the symmetric structure is more stable.

We also found that there is a remarkable difference in the size distribution of the nanovoids in the samples implanted with the two different doses. As the dose is increased to 2×10^{17} from 1×10^{17} ions/ cm^2 , the average size of the nanovoids, calculated from the TEM images, decreased rapidly from 18.7 to 11.2 nm. This indicates that the nanovoids shrink with increasing dose. Actually, by comparing the TEM images of the samples implanted with doses of 1×10^{17} and 2×10^{17} ions/ cm^2 , it is found that some nanovoids had been filled up by Ag atoms, as seen in Fig. 2. The inner free surfaces of the nanovoids with

TABLE I. Total energies of Ag nanoclusters by molecular mechanics calculations. Ag_{160} (I): the nanovoid and nanocluster are concentric, Ag_{160} (II): the center of nanovoid shifted 0.07 nm along the x axis from the center of the nanocluster. After calculations, the structures are optimized and the energies decrease to the lowest calculated values.

	Ag_{12}		Ag_{160}		$\text{Ag}_{12} + \text{Ag}_{160}$		$\text{Ag}_{12}@Ag_{160}$ (after calculation)	
	Ag_{12}	Ag_{160}	Ag_{160} (I)	Ag_{160} (II)	$\text{Ag}_{12} + \text{Ag}_{160}$ (I)	$\text{Ag}_{12} + \text{Ag}_{160}$ (II)	$\text{Ag}_{12}@Ag_{160}$ (I)	$\text{Ag}_{12}@Ag_{160}$ (II)
Total energy [kcal/mol]	1508	25 302	25 581		26 810	27 089	26 747	27 019
Total energy [kcal/mol · atom]	125.7	158.1	160.0		155.9	157.5	155.5	157.1

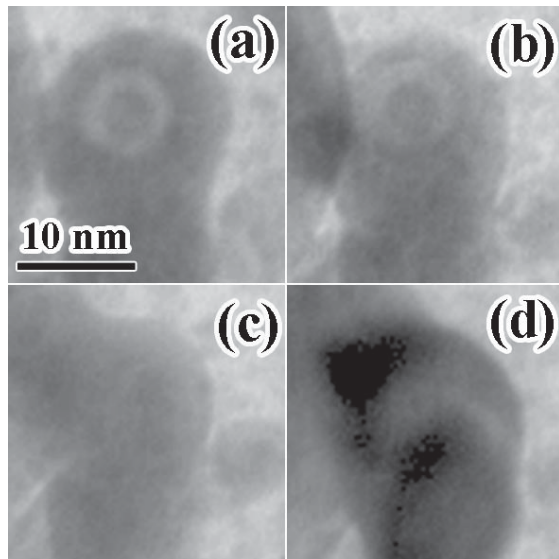


FIG. 5. *In situ* TEM images for the sample implanted by 200 keV, 2×10^{17} Ag⁺ ions/cm² after annealing at 600 °C for 31 (a), 32 (b), 33 (c), and 34 (d) min.

dangling bonds have been proved to be able to effectively trap subsequently implanted and interstitial atoms due to extra high surface energy and athermal activation of the energetic-beam irradiation, leading to the shrinkage of the nanovoids [15]. The growth and shrinkage of nanovoids during ion implantation was a result of the competition between the aggregation of irradiation-reduced vacancies and the trap of the implanted Ag atoms. At the initial stage, the aggregation of vacancies played a decisive role to form nanovoids. When the nanovoids become larger and the number of dangling bonds increase greatly, trapping of Ag atoms become dominant.

The *in situ* observation of the evolution of sandwiched structure Ag nanoclusters was carried out in TEM to study the influence of annealing. Figures 5(a)–5(d) show the TEM images of the 2×10^{17} Ag ions/cm² implanted sample annealed at 600 °C for different times. Clearly, the size of nanovoid grew to 18.2 nm after annealed for 31 min comparing to the 16.6 nm for 30 min, while the core stayed stable inside the nanovoid. Then the size shrunk to 4.9 nm after being annealed for 32 min and the core was absorbed by the inner wall of the nanoshell. Finally, the nanovoid disappeared after annealing for 33 min. This *in situ* TEM observation is consistent with the previous *ex situ* TEM observation of Cu nanoclusters with nanovoids [12].

In conclusion, we have observed nanovoid-containing and sandwiched structure of nanocluster-nanovoid-nanocluster Ag nanoclusters in SiO₂ by ion implantation with controlled doses. The nanovoids grow up and then shrink with the increasing dose as a result of the competition between the aggregation of vacancies and the trap of

Ag atoms. The *in situ* TEM observation of the sandwiched structure nanoclusters during annealing also found this evolution. The stability of the sandwiched Ag nanoclusters was confirmed by molecular mechanics calculations. These results help to understand the mechanism of the formation of nanovoids and the evolution with increasing dose. They also provide a method to form and tailor hollow nanoclusters and to capture atoms or clusters in them.

The authors thank Professor R. H. Wang for useful discussions, Professor Y. F. Yan for critical reading of the manuscript, and Dr. H. B. Chen in helping prepare the samples. This work was supported by the Natural Science Foundation of China (No. 10375044 and No. 10435060) and by the Key Project of the Chinese Ministry of Education (No. 104122).

*Corresponding author.

Electronic address: czjiang@whu.edu.cn

- [1] X. Y. Gao, J. S. Zhang, and L. Zhang, *Adv. Mater.* **14**, 290 (2002).
- [2] G. Schneider, and G. Decher, *Nano Lett.* **4**, 1833 (2004).
- [3] E. Prodan, C. Radloff, N. J. Halas, and P. Nordlander, *Science* **302**, 419 (2003).
- [4] R. C. Jin, Y. C. Cao, E. C. Hao, G. S. Metraux, G. C. Schatz, and C. A. Mirkin, *Nature (London)* **425**, 487 (2003).
- [5] A. Meldrum, L. A. Boatner, and C. W. White, *Nucl. Instrum. Methods Phys. Res., Sect. B* **178**, 7 (2001).
- [6] J. C. Pivin, and G. Rizza, *Thin Solid Films* **366**, 284 (2000).
- [7] L. E. Rehn, R. C. Birtcher, S. E. Donnelly, P. M. Baldo, and L. Funk, *Phys. Rev. Lett.* **87**, 207601 (2001).
- [8] H. Hosono, *Phys. Rev. Lett.* **74**, 110 (1995).
- [9] S. Roorda, T. van Dillen, A. Polman, C. Graf, A. van Blaaderen, and B. J. Kooi, *Adv. Mater.* **16**, 235 (2004).
- [10] J. J. Penninkhof, C. Graf, T. van Dillen, A. M. Vredenberg, A. van Blaaderen, and A. Polman, *Adv. Mater.* **17**, 1484 (2005).
- [11] A. Meldrum, *J. Mater. Res.* **16**, 2670 (2001).
- [12] F. Ren, C. Z. Jiang, C. Liu, and J. B. Wang, *Appl. Phys. Lett.* **88**, 183114 (2006).
- [13] G. Mattei, G. De Marchi, C. Maurizio, P. Mazzoldi, C. Sada, and V. Bello, *Phys. Rev. Lett.* **90**, 085502 (2003).
- [14] G. Mattei, V. Bello, P. Mazzoldi, G. Pellegrini, C. Sada, C. Maurizio, and G. Battaglin, *Nucl. Instrum. Methods Phys. Res., Sect. B* **240**, 128 (2005).
- [15] X. F. Zhu, *J. Phys. Condens. Matter* **15**, L253 (2003).
- [16] T. Ohtsuki, K. Ohno, K. Shiga, Y. Kawazo, e, Y. Maruyama, and K. Masumoto, *Phys. Rev. Lett.* **81**, 967 (1998).
- [17] E. Dietel, A. Hirsch, B. Pietzak, M. Waiblinger, K. Lips, A. Weidinger, A. Gruss, and K. P. Dinse, *J. Am. Chem. Soc.* **121**, 2432 (1999).
- [18] A. Kaplan, Y. Manor, A. Bekkerman, B. Tsipinyuk, E. Kolodney, *Int. J. Mass Spectrom.* **228**, 1055 (2003).